

CHARACTERIZATION OF HIGH SPEED DIGITAL VIDEO CAMERA*

by

ASHER GELBART**

ROCHESTER INSTITUTE OF TECHNOLOGY

ROCHESTER, NEW YORK

BRIAN RODRICKS

EXPERIMENTAL FACILITIES DIVISION

ARGONNE NATIONAL LABORATORY

ARGONNE, ILLINOIS

The submitted manuscript has been created by the University of Chicago as Operator of Argonne National Laboratory ("Argonne") under Contract No. W-31-109-ENG-38 with the U.S. Department of Energy. The U.S. Government retains for itself, and others acting on its behalf, a paid-up, nonexclusive, irrevocable worldwide license in said article to reproduce, prepare derivative works, distribute copies to the public, and perform publicly and display publicly, by or on behalf of the Government.

*Work performed at Argonne National Laboratory, a contract Laboratory of the United States Department of Energy

**Participant in the Summer 1996 Student Research Participation Program. This program is coordinated by the division of Educational Programs.

DRAFT

Detector Characterization

The characterizations developed in this paper have been performed on a high speed digital video camera designed and built by the Detector Development Group at the Advanced Photon Source, Experimental Facilities Division. The camera is based around the Thomson TH7895AH detector, which is a 2-output scientific CCD. Each output (channel 1, and channel 2) of the CCD is clocked out at 13.3 MHz. The data undergoes correlated double sampling after which it is digitized to 12 bits using commercially available Analog-to-Digital converters. The throughput of the system translates to 60 MB/sec that is either stored directly in a PC or transferred to a custom designed VXI module holding 512 MB of DRAM.

Using visible light, the photon transfer technique^[1,2] has been utilized to yield detector characterizations of linearity, dark current, electronic read noise, full well saturation levels, signal to noise ratio, dynamic range, and electrons/analog-to-digital unit. All of these parameters are obtained from one procedure, in which images are captured at a series of integration times with a uniform light source.

The resolving power in the form of a Modulation Transfer Function (MTF) has been characterized using the knife edge technique^[3].

DRAFT

Linearity:

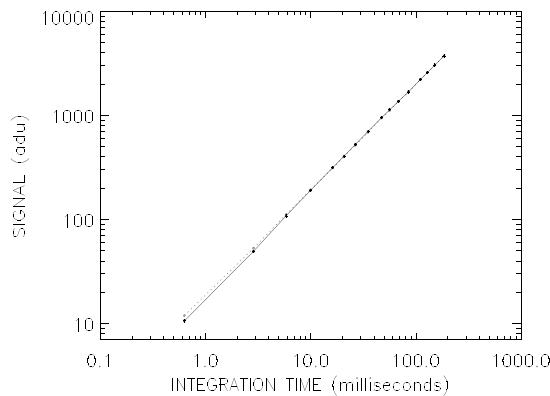


Figure 1. Linearity for channel 1 (solid) and channel 2 (dotted).

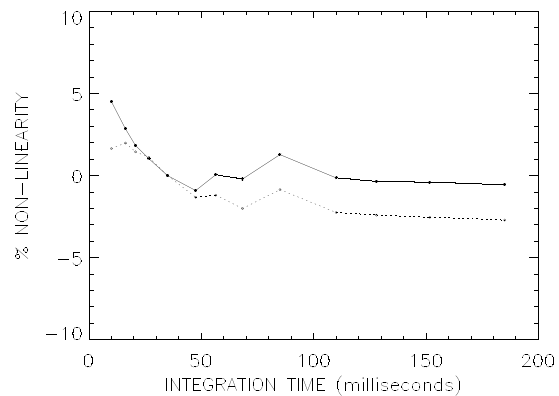


Figure 2. Linearity Residuals

The primary characterization performed on the camera was a test for linearity, which also provides data applicable to a number of other characterization attributes.

The test for linearity was performed by capturing a series of images of a uniformly illuminated field at varying integration times. A high intensity LED, diffused with an 8" diameter integrating sphere and ground glass, was used as the light source. With the voltage to the light source held constant, integration times were bracketed from 1 to 250 milliseconds with a waveform generator that triggered the readout of the camera. The waveform generator also extinguished the LED during the CCD read time, thus acting as shutter to prevent extraneous exposure during readout.

For each integration time, two image frames were captured along with two dark frames. The two frames at each exposure level are necessary for calculating noise, which will be discussed later. For the linearity characterization, data points are generated by subtracting one dark frame from one image frame (to remove offset dark current) and calculating the mean over a 20 x 20 pixel region at the center of each of the two image outputs. Although each output of the CCD leads to identically configured circuitry, there is a potential for small variations between the two channels due to component tolerances. Figure 1 shows the

DRAFT

linearity of the camera for each output channel. In Figure 2, the results are expanded to show small nonlinearities using the following equation:

$$LR(\%) = 100(1 - T_e S_m / T_{em} S)$$

where: T_e = Integration time

T_{em} = Integration time to achieve mid-signal

S = Signal (analog-to-digital units, “adu”)

S_m = $S(\text{adu})$ at T_{em}

The results indicate that the camera's response to radiation is linear to within 3% over the entire, 12-bit dynamic range.

DRAFT

Photon Transfer Function:

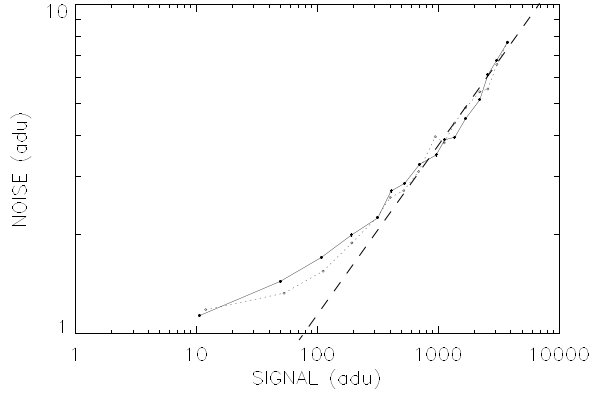


Figure 3. The Photon Transfer Curve for both outputs channels. The straight dashed line is an extrapolation of the straight portion of the curve. The camera gain constant, K , is approximated by the signal intercept of this line.

The photon transfer curve is a plot of random noise, σ_s , as a function of the signal (adu). The signal noise, σ_s , is defined as the square root of the variance of the signal, with the fixed pattern noise removed. Fixed pattern noise is removed by subtracting two images taken back to back at the same exposure level. The variance is computed over a region of the differenced image and divided by two (because the rms noise increases by the square root of 2 when two identical frames are either added or subtracted).

According to Poisson statistics, the noise, σ_s , is proportional to the square root of the signal when outside the single photon counting regime. It follows, that the photon transfer curve plotted on a log-log plot should yield a slope of 1/2. Because the photon transfer curve includes both the read noise, σ_r , and the shot noise, σ_s , the curve is nonlinear at low signals where the dark current noise has a considerable contribution, and becomes linear as the shot noise of the signal overpowers the read noise.

Figure 3 is the photon transfer curve, showing the anticipated slope of 0.5 for the straight line portion of the curve to within +/- 15%.

DRAFT

Electrons per Analog-to-Digital Unit:

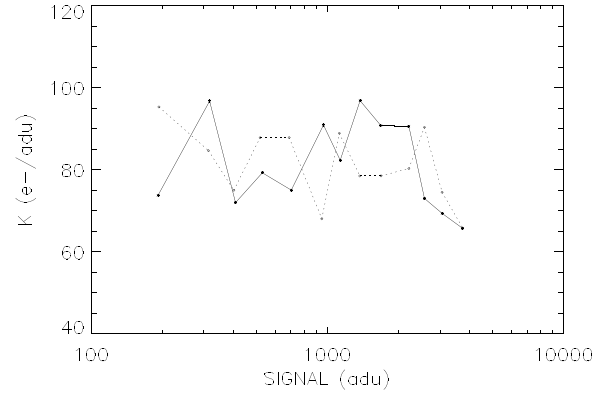


Figure 4. Camera gain constant, K (e-/adu) for both output channels.

The camera gain constant, K , represents number of electrons per analog digital unit (e-/adu):

$$K = S(\text{adu}) / (\sigma_s^2 - \sigma_r^2)$$

where: K = electrons/S(adu)

S = signal (analog digital units)

σ_s^2 = variance of the signal

σ_r^2 = variance of the dark current

Figure 4 shows the “constant,” K , calculated for each data point using the above equation. The variances, σ_s^2 , and σ_r^2 are both generated as described above by differencing identical frames. Being a constant, this should be a straight horizontal line. The results indicate an average value for K of 79.45 electrons/adu with a +/- 15% fluctuation.

K can also be approximated from the photon transfer curve. It can be shown that an extrapolation

DRAFT

of the straight portion of the photon transfer curve (see Figure 3) will intercept the signal axis at the value of K:

$$K = S(\text{adu})/(\sigma_s^2 - \sigma_r^2)$$

The variance of the dark current, σ_r^2 , is small in comparison to the variance of the signal, σ_s^2 . Considering the contribution of σ_r^2 to be negligible, as it is for the straight portion of the curve, then:

$$K = S(\text{adu})/(\sigma_s^2)$$

It follows that when the signal noise is equal to 1 (at the signal axis intercept on the photon transfer curve):

$$K = S(\text{adu})$$

The extrapolated straight line intercept of the S(adu) axis indicates that K is approximately 80 e-/S(DN), which agrees with the values calculated in Figure 4.

This value is also consistent with the data specifications for the Thomson TH7895AH which predict a value between 68 and 123 e-/adu.

Dark Current Noise (Read Noise Floor):

DRAFT

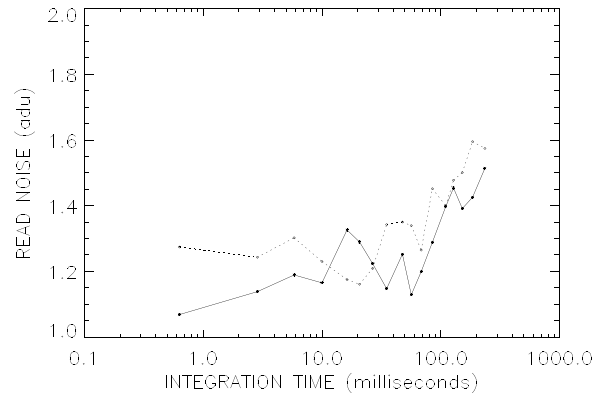


Figure 5. Read noise as a function of integration time for both output channels.

Because the camera is maintained at room temperature, the read noise is expected to rise with increasing integration time due to thermal effects. Dark current noise, σ_r , is calculated as square root of $1/2$ the variance of two differenced dark images, as described above. Figure 5 shows dark current noise as a function of integration time. The dark current RMS noise remains below 1.6 for integration times up to 250 milliseconds with noise values as low as 1.05.

DRAFT

Dynamic Range:

The Dynamic Range is defined as the digital number at full well divided by the rms noise of the read noise floor:

$$DR = FW/\sigma_r$$

where: FW = ADU at full well capacity

σ_r = the read noise measured

The calculated dynamic range is 3900 (4095/1.05), meaning that the camera can resolve intensity changes as small as one part in 3900.

Signal to Noise Ratio:

The signal to noise ratio^[1,4] is defined as:

$$S/N = S/\sigma_s$$

Assuming negligible read noise, and a quantum yield of 1, the equation reduces to:

$$S/N = S/(S)^{1/2} = S^{1/2}$$

S/N is often given in decibels, where the conversion is defined as:

DRAFT

$$\text{dB} = 20 \log (S/N)$$

When calculating signal to noise ratios, the signal must be in terms of electrons, because the S/N changes depending on the energy of the radiation. The gain constant, K, is used to convert adu to units of electrons.

We will use the average value of K , 79.45 e-/adu, rounded to 80 e-/adu.

Using the ideal case, $S/N = S^{1/2}$:

$$S/N = (4095 \text{ adu} * 80 \text{ e-/adu})^{1/2} = 572 = 55 \text{ dB}$$

Using actual measured data points for maximum signal and noise:

$$S/N = (3835 \text{ adu} * 80 \text{ e-/adu}) / (7.68 \text{ adu} * 80 \text{ e-/adu}) = 499 = 54 \text{ dB}$$

The measured S/N varies from the ideal calculation by less than 2%.

DRAFT

Modulation Transfer Function (MTF):

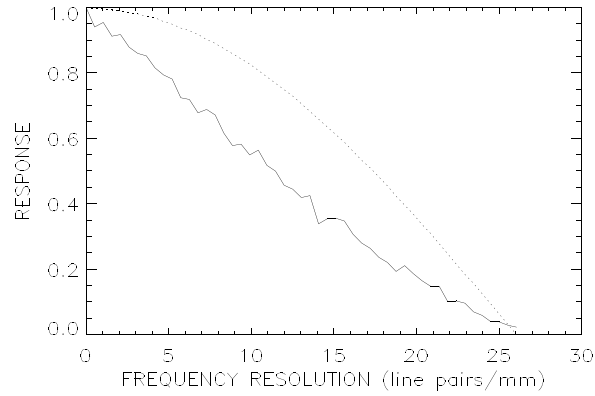


Figure 6. Modulation Transfer Function (MTF).
Solid line is actual MTF. Dotted line is ideal MTF.

The MTF was calculated using the Knife Edge technique developed for electronic imaging devices by Reichenbach, et al^[3]. The MTF is a plot of contrast (i.e. visual contrast between dark to light fluctuations) as a function of frequency resolution in line pairs per mm.

The MTF is generated from imaging a knife edge onto the detector. A profile of the edge is called the edge trace function, $e(x)$. The first derivative of the edge trace function gives the line spread function, $L(x)$. The Optical Transfer Function (OTF) is the fourier transform of the line spread function, and the MTF is defined as the absolute value of the OTF:

$$e(x) = \text{edge trace function}$$

$$L(x) = f[e(x)] = \text{line spread function}$$

$$\text{OTF} = \text{FFT}[L(x)] = \text{optical transfer function}$$

DRAFT

$MTF = |OTF| = \text{modulation transfer function}$

The knife edge was generated on high contrast lithographic film, using standard lithography. The film was taped directly to the fiber optic face plate coupled to the detector. A high intensity LED was used as a light source. The beam was collimated using a pinhole and a lens positioned one focal length from the pinhole. One image was used to generate multiple edge trace functions. The MTF was calculated independently for 80 rows and averaged. Because the knife edge was intentionally placed at a slight angle with respect to the fixed pixel grid, the averaging served to increase effective sampling across the edge and to reduce noise. Another method discussed by Reichenbach, et al^[3] achieves a similar effect by estimating edge locations to “sub-pixel accuracy,” and shifting to register the lines, thus generating one scan line with “super-resolution” (resolution higher than the sampling rate) from which the MTF is calculated.

Figure 6 is the MTF generated for our camera. The detector, with a 1:1 fiber optic face plate, is capable of resolving 12 line pairs per mm at 50% contrast. This resolution corresponds to the width of 4.4 pixels ($1/12 \text{ line pairs per mm} = 83 \text{ microns per cycle}$; $83 \text{ microns}/19 \text{ microns per pixel} = 4.4 \text{ pixels}$) such that one cycle, (light to dark to light fluctuation) spanning 4.4 pixels would be imaged to 50% its physical contrast. The dotted line is the ideal MTF generated from a digitally created, one bit, edge.

DRAFT

References:

1. Janesick, J.R., "Charge-Coupled Devices, Cameras, and Applications," UCLA Engineering 881.150 short course, section 2, Oct. 9-12, 1995.
2. J.R. Janesick, P.K. Klassen, Tom Elliot, "Charge-Coupled-Device Charge-Collection Efficiency and the Photon-Transfer Technique," Opt. Eng. 26(10), 972-989 (1987).
3. E.C. Reichenbach, S.K. Park, R. Narayanswamy, "Characterizing digital image acquisition devices," Opt. Eng. 30(2), 170-177 (1991).
4. Mullikin, J.C., L.J. van Vliet, H. Netten, F.R. Boddeke, G. van der Feltz, I.T. Young, "Methods for CCD Camera Characterization," SPIE (2173), 73-84 (1994).